Spin-State Variation in Solid State and Solution of Mononuclear Iron(II) 1,4,7-Trimethyl-1,4,7-triazacyclonane Complexes

David W. Blakesley, Sonha C. Payne, and Karl S. Hagen*

Department of Chemistry, Emory University, Atlanta, Georgia 30322

Received May 20, 1999

The series of mononuclear iron(II) complexes with the tridentate macrocycle Me_3tacn have been prepared (Me_3tacn = 1,4,7-trimethyl-1,4,7-triazacyclonane). A purple, spin-crossover complex $[Fe(Me_3tacn)(MeCN)_3](CF_3SO_3)_2$ (**1**−OTf) forms in acetonitrile but readily loses MeCN ligands to form a colorless high-spin complex $Fe(Me_3tacn)(OTf)_2$ (**2**). The BPh_4^- salt of **1** is stable to loss of MeCN and remains purple even under a vacuum. Methylene chloride solutions of $Fe(OTf)_2$ and Me_3tacn afford crystals of $[Fe(Me_3tacn)(MeCN)_2(OTf)](OTf)$ (**3**). Crystallization of **1**−OTf in the presence of water affords a colorless high-spin complex, $Fe(Me_3tacn)(H_2O)(CF_3SO_3)_2$ (**4**), that exists as a pair of molecules bridged by hydrogen bonds between the coordinated water and the two bound triflate anions of the inversion-related partner. The crystallographic parameters are the following. **1**−BPh_4: $C_{63}H_{70}B_2Fe$, monoclinic, $P2_1/c$, $a = 18.360(1)$ Å, $b = 11.761(1)$ Å, $c = 25.754(2)$ Å, $\beta = 90.72(1)°$, $Z = 4$. **3**: $C_{16}H_{29}Cl_2F_6FeN_5O_6S_2$, triclinic group $P\bar{1}$, $a = 8.500(1)$ Å, $b = 11.421(2)$ Å, $c = 15.677(2)$ Å, $\alpha = 92.23(1)°$, $\beta = 94.79(1)°$, $\gamma = 97.03(1)°$, $Z = 2$. **4**: $C_{20}H_{18}F_6FeN_4O_6S_2$, monoclinic, $P2_1/n$, $a = 11.253(3)$ Å, $b = 12.624(5)$ Å, $c = 14.683(5)$ Å, $\beta = 94.02(2)°$, $Z = 4$. Variable temperature visible spectra and ^{1}H NMR spectra of solutions of both **1**−OTf and **1**−BPh_4 exhibit low-spin, high-spin crossover behavior, whereas **2**, **3**, and **4** remain high-spin in solution. The extensive role of coordinated triflate as a terminal and/or bridging ligand as well as a counteranion is demonstrated by variable temperature ^{19}F NMR spectra.

Introduction

The first generation of model complexes for non-heme diiron proteins were μ-oxo, bis(μ-carboxylato) diiron(III) complexes capped by the tridentate ligands Tp ($HBpz_3^-$) or tacn (1,4,7-triazacyclononane). A major drawback of these ligands for the synthesis of diiron(II) complexes as models for the active, reduced forms of the proteins is the formation of stable iron(II) bis(ligand) complexes instead of the desired binuclear model complexes. For example, formation of the neutral complex $Fe(Tp)_2$ interfered with the syntheses of binuclear iron(II) model complexes of non-heme proteins with this ligand.[1] Similarly, tacn forms a pale-blue sandwich complex, $[Fe(tacn)_2]^{2+}$, in preference to a binuclear species.[2,3]

The choice of appropriate multidentate ligands for iron(II) is still very important. Six-coordinate iron(II) complexes may be diamagnetic, low-spin ($^1A_1$, LS), paramagnetic, high-spin ($^5T_2$, HS), or exhibit a temperature, light, or pressure induced LS ↔ HS transition that depends on the relative ligand field stabilization. Solid-state properties of complexes that exhibit LS ↔ HS transitions is an active area of research that has been extensively reviewed.[4−10] The reactivity of iron(II) complexes in solution is intimately related to the spin state of the metal centers in the complex. LS six-coordinate iron(II) complexes form with sterically unencumbered multidentate chelating ligands, that is, Tp and tacn, which hinder subsequent ligand substitution reactions at the metal centers. However, Kitajima and co-workers have shown that bulky isopropyl substituents on the ligand not only inhibit formation of the sandwich complex but also stabilize the HS state in mononuclear and binuclear model complexes.[11] The *N*,*N*′,*N*″-trimethyl derivative of the triazacyclonane ligand Me_3tacn was employed for the synthesis of $[Fe_2(OH)(OAc)_2(Me_3tacn)_2]^+$, the first truly representative model of the iron(II) state of hemerythrin.[12] Presumably, the bulky methyl groups prevent formation of the undesired sandwich complex $[Fe(Me_3tacn)_2]^{2+}$. This ligand has also been used for the preparation of other iron(II) complexes, including the mononuclear $Fe(Me_3tacn)(NO)(N_3)_2$, binuclear $[\{Fe(Me_3tacn)L_2\}_2]$ (L = NCS^-, NCO^-, and N_3^-),[13] and the mixed-valence Fe(II)Fe(III) dimers $[Fe_2(OH)_3(Me_3tacn)_2]^{2+}$, $[Fe_2(OH)(Me_3CCO_2)_2(Me_3tacn)_2]^{2+}$,[14] and $[Fe_2O(Me_3CCO_2)_2(Me_3tacn)_2]^{2+}$.[15] To understand the chemistry of diiron(II) cores in biomolecules,

(1) (a) Armstrong, W. H.; Lippard, S. J. *J. Am. Chem. Soc.* **1983**, *105*, 4838−4838. (b) Armstrong, W. H.; Spool, A.; Papaefthymiou, G. C.; Frankel, R. B.; Lippard, S. J. *J. Am. Chem. Soc.* **1984**, *106*, 3653−3667.
(2) Boeyens, J. C. A.; Forbes, A. G. S.; Hancock, R. D.; Wieghardt, K. *Inorg. Chem.* **1985**, *24*, 2926−2931.
(3) Hagen, K. S.; Diebold, A.; Brewer, M. Manuscript in preparation.
(4) Goodwin, H. A. *Coord. Chem. Rev.* **1976**, *18*, 293−325.
(5) Toftlund, H. *Coord. Chem. Rev.* **1989**, *94*, 67−108.
(6) Gütlich, P. *Struct. Bonding* **1981**, *44*, 83−195.
(7) Gütlich, P.; Hauser, A. *Coord. Chem. Rev.* **1990**, *97*, 1−22.
(8) König, E. *Struct. Bonding* **1991**, *76*, 51−152.
(9) Hauser, A. *Coord. Chem. Rev.* **1991**, *111*, 275−290.
(10) Gütlich, P.; Hauser, A.; Spieling, H. *Angew. Chem., Int. Ed. Engl.* **1994**, *33*, 2024−2054.
(11) Kitajima, N.; Dolman, W. B. *Prog. Inorg. Chem.* **1995**, *43*, 419−531.
(12) (a) Chaudhuri, P.; Wieghardt, K.; Nuber, B.; Weiss, J. *Angew. Chem.* **1985**, *97*, 774−775. (b) Hartman, J. A. R.; Rardin, R. L.; Chaudhuri, P.; Pohl, K.; Wieghardt, K.; Nuber, B.; Weiss, J.; Papaefthymiou, G. C.; Frankel, R. B.; Lippard, S. J. *J. Am. Chem. Soc.* **1987**, *109*, 7387−96.
(13) Pohl, K.; Wieghardt, K.; Nuber, B.; Weiss, J. *J. Chem. Soc., Dalton Trans.* **1987**, 187−92.
(14) Boseki, U.; Humble, H.; Thomas, W.; Bill, E.; Wieghardt, K. *Angew. Chem., Int. Ed. Engl.* **1996**, *34*, 2642−5.
(15) Cohen, J. D.; Payne, S. C.; Hagen, K. S.; Sanders-Loehr, J. *J. Am. Chem. Soc.* **1997**, *119*, 2960−2961.

10.1021/ic990584+ CCC: $19.00
Published on Web 04/13/2000

we have prepared and studied the reactivity of the small molecule, binuclear iron(II) complexes $[Fe_2(OH)(R_3CCO_2)_2(Me_3tacn)_2]^+$ (R = F,[16] Me,[16b] Ph[15]). We noticed that the chemistry of iron(II) and Me_3tacn in the absence of strongly basic ligands (e.g., hydroxide, carboxylates) is also very rich.

For example, we report here that the complexation of acetonitrile to the $Fe(Me_3tacn)^{2+}$ moiety results in formation of the LS ↔ HS crossover complex $[Fe(Me_3tacn)(CH_3CN)_3]^{2+}$. This complex exhibits spin-crossover behavior and ligand substitution equilibria in solution that have been studied using variable temperature multinuclear NMR spectroscopy. Related solution chemistry can be found for iron(II) complexes of the tetradentate ligand tris(2-pyridylmethyl)amine[17,18] and a saturated tetradentate macrocyclic ligand.[19] This spin-crossover behavior contrasts with that of systems involving only one or two multidentate ligands such as $[Fe((NH_2)_2sar)]^{2+}$,[20] $[Fe(tacn)_2]^{2+}$,[3] or $FeTp_2$ where ligand substitution requires the removal of the sexadentate ligand or stepwise deligation of a tridentate ligand.

Experimental Section

Synthetic Methods. All reactions were performed under an inert atmosphere in a N_2-filled glovebox or Schlenk line unless otherwise specified. Triflic acid was used as obtained from 3M Co. $Fe(OTf)_2 \cdot 2CH_3CN$ was prepared under a dinitrogen atmosphere by reacting finely divided Fe metal and triflic acid in dry acetonitrile, crystallizing the product by adding ether, and drying the product at room temperature in a vacuum. Anhydrous grade acetonitrile was purchased from Aldrich and stored under dry dintrogen in a glovebox. All other solvents were distilled or dried over sieves and degassed.

Physical Measurements. ^1H NMR spectra were recorded on a General Electric QE-300, a Nicolet NT-360, a Varian Inova 400, or a General Electric GN-500 spectrometer in CD_3CN, $(CD_3)_2SO$, CD_2Cl_2, or $CDCl_3$ and referenced to tetramethylsilane. ^2H and ^{19}F NMR spectra were referenced to $CDCl_3$ (at 7.26 ppm) and $CFCl_3$, respectively. Electronic absorption spectra were collected on a Shimadzu UV-3101PC, UV−vis−NIR scanning spectrophotometer. Room-temperature magnetic moments of powder samples were measured using an Evans magnetic susceptibility balance (Johnson Matthey, model MSB-1) calibrated with $Hg[Co(SCN)_4]$ using Pascal's constants for diamagnetic corrections. Variable temperature solid-state magnetic measurements were performed on a superconducting quantum interference device (SQUID) susceptometer. Magnetic moments in solution were measured using the Evans method on either the 300 or 500 MHz NMR spectrometer.[21] Elemental analyses were performed by Atlantic Microlabs, Inc. Atlanta, GA.

$[Fe(Me_3tacn)(MeCN)_3](OTf)_2$ (1−OTf). Neat Me_3tacn (0.342 g, 2.00 mmol) was added to a colorless solution of $Fe(OTf)_2 \cdot 2MeCN$ (0.872 g, 2.00 mmol) in 3 mL of acetonitrile to give a dark-purple solution. Diethyl ether was added to the reaction mixture, and formation of a purple precipitate was observed. $[Fe(Me_3tacn)(MeCN)_3](OTf)_2$ was isolated as a purple powder (0.999 g, 77%), which was collected by vacuum filtration, washed with diethyl ether, and dried in vacuo. Large, dark-purple crystals were obtained by recrystallization from acetonitrile/diethyl ether. These lose their coordinated MeCN as shown by the elemental analysis. Anal. Calcd for $C_{11}H_{21}F_6FeN_3O_6S_2 \cdot 0.2MeCN$: C, 25.67; H, 4.08; N, 8.40. Found: C, 25.5; H, 4.4; N, 8.7.

$Fe(Me_3tacn)(OTf)_2$ (2−OTf). Neat Me_3tacn (0.342 g, 2.00 mmol) was added to a colorless solution of $Fe(OTf)_2 \cdot 2MeCN$ (0.872 g, 2.00 mmol) in 3 mL of THF to give a pale-yellow solution. Diethyl ether (2 mL) was added, and the reaction mixture was placed in the freezer. After 2 weeks at −20 °C, $Fe(Me_3tacn)(OTf)_2$ (0.891 g, 85%) was isolated as large colorless plates that were collected by vacuum filtration, washed with diethyl ether, and dried in vacuo. Anal. Calcd for $C_{11}H_{21}F_6FeN_3O_6S_2$: C, 25.15; H, 4.03; N, 8.00. Found: C, 26.5; H, 4.0; N, 7.8. Calcd for $\mathbf{1}-OTf \cdot {}^1/_4Et_2O$: C, 26.50, H, 4.36, N, 7.73.

$[Fe(Me_3tacn)(MeCN)_2(OTf)](OTf)$ (3). The reaction of $Fe(OTf)_2 \cdot 2MeCN$ and 2.0 equiv of Me_3tacn in CH_2Cl_2 followed by layering pentane on the solution affords a few purple crystals of **1**−OTf and some large colorless crystals that have been shown by X-ray crystallography to be $[Fe(Me_3tacn)(MeCN)_2(OTf)](OTf) \cdot CH_2Cl_2$ (**3**$\cdot CH_2Cl_2$). These crystals are unstable to loss of acetonitrile and could not be characterized by other techniques.

$[Fe(Me_3tacn)(MeCN)_3](BPh_4)_2$ (1−BPh_4). Neat Me_3tacn (0.342 g, 2.00 mmol) was added to a colorless solution of $Fe(OTf)_2 \cdot 2MeCN$ (0.872 g, 2.00 mmol) in 10 mL of acetonitrile to give a dark-purple solution. A pink solution of sodium tetraphenylborate (1.369 g, 4.00 mmol) in 5 mL of acetonitrile was added to the purple reaction mixture. In less than 5 min, formation of dark-purple crystals was observed. After 1 day at room temperature, dark-purple crystals of $[Fe(Me_3tacn)(MeCN)_3](BPh_4)_2$ (1.630 g, 83%) were collected by vacuum filtration, washed with diethyl ether, and dried in vacuo. Large, dark-purple crystals suitable for study by X-ray diffraction were obtained by slow cooling of a hot acetonitrile solution. Anal. Calcd for $C_{63}H_{70}B_2FeN_6$: C, 76.53; H, 7.14; N, 8.50. Found: C, 76.3; H, 7.1; N, 8.4.

$Fe(Me_3TACN)(H_2O)(OTf)_2$ (4). An amount of 200 mg of $[Fe(Me_3tacn)(MeCN)_3](OTf)_2$ was dried under vacuum, affording 164 mg of nearly colorless $Fe(Me_3tacn)(OTf)_2$. This was treated with 7 mL of anhydrous THF. Some of the white solid remained but rapidly dissolved on addition of 6 μL of H_2O. The THF was removed under vacuum, affording a white solid. Crystals were grown by dissolving 33 mg of this product in 1 mL of THF in a vial that was placed in a larger vial containing 3 mL of Et_2O.

Crystallographic Studies. Crystals of **1**−BPh_4, **3**, and **4** suitable for X-ray crystallographic analysis were obtained as described in the Experimental Section (vide supra). All crystals were coated with a viscous oil and mounted with superglue on the end of glass fibers. The diffraction intensities were collected using Cu Kα graphite monochromated radiation on a Siemens P4/RA single-crystal X-ray diffractometer. During data collection the intensities of three representative reflections, monitored every 97 reflections, indicated a decay of 9%, 16%, and 0% for **1**−BPh_4, **3**, and **4**, respectively. The structures were solved by direct methods (SHELXS-86) and difference Fourier methods and refined by full-matrix least-squares methods (SHELXTL). All non-hydrogen atoms were refined with anisotropic thermal parameters. Hydrogen atoms were included and placed at calculated positions. The details of the data collection and refinement procedures are given in Table 1 and in Supporting Information in CIF format. Selected bond lengths and angles are given in Tables 2 and 3.

Results and Discussion

Syntheses of Iron(II) Complexes. Iron(II) triflate is our starting material of choice. It is simply prepared by reacting finely divided iron metal with triflic acid in acetonitrile. Very pale-green crystals of $[Fe(MeCN)_4](OTF)_2$ can be isolated on addition of diethyl ether to acetonitrile solutions. Two of the coordinated acetonitrile ligands are readily lost under vacuum to form a white powder that analyzes as $Fe(OTF)_2 \cdot 2MeCN$.[22] Triflate is a convenient anion for iron(II) complex formation because halide ions would coordinate to the metal, and perchlorate ion, the weakly coordinating anion that is traditionally favored, forms explosive salts.[23] Triflate is a weakly coordinating

(16) (a) Lachicotte, R.; Kitaygorodskiy, A.; Hagen, K. S. *J. Am. Chem. Soc.* **1993**, *115*, 8883−8884. (b) Lachicotte, R. J. Ph.D. Thesis, Emory University, Atlanta, GA, 1995.
(17) Zang, Y.; Kim, J.; Dong, Y. H.; Wilkinson, E. C.; Appelman, E. H.; Que, L. *J. Am. Chem. Soc.* **1997**, *119*, 4197−4205.
(18) Diebold, A.; Hagen, K. S. *Inorg. Chem.* **1998**, *37*, 215−223.
(19) Dabrowiak, J. C.; Merrell, P. H.; Busch, D. H. *Inorg. Chem.* **1972**, *9*, 1979−1988.
(20) (a) Martin, L. L.; Hagen, K. S.; Hauser, A.; Martin, R. L.; Sargeson, A. M. *J. Chem. Soc., Chem. Commun.* **1988**, 1313−1315. (b) Martin, L. L.; Martin, R. L.; Sargeson, A. M. *Polyhedron* **1994**, *13*, 1969−80. (c) Martin, L. L.; Martin, R. L.; Murray, K. S.; Sargeson, A. M. *Inorg. Chem.* **1990**, *29*, 1387−94.
(21) Evans, D. F. *J. Chem. Soc.* **1959**, 2003−2005.
(22) Hagen, K. S. Manuscript in preparation.

Table 1. Crystallographic Data for the Complexes **1**-BPh_4, **3**, and **4**

	1-BPh_4	**3**	**4**
empirical formula	$C_{63}H_{70}B_2FeN_3$	$C_{11}H_{23}F_6FeN_3O_7S_2$	$C_{16}H_{29}Cl_2F_6FeN_5O_6S_2$
fw	988.72	543.29	692.31
λ, Å	1.541 78 (Cu Kα)	1.541 78 (Cu Kα)	1.541 78 (Cu Kα)
space group, no.	$P2_1/c$, 14	$P2_1/n$, 14	$P\bar{1}$, 2
Z	4	4	2
μ, cm^{-1}	2.505	8.57	7.66
temp, °C	−30, 67, 90	−62	−100
a, Å	18.360(1), 18.422(2), 18.4560(9)	11.253(3)	8.500(1)
b, Å	11.761(1), 11.808(2), 11.823(1)	12.624(5)	11.421(2)
c, Å	25.752(2), 26.110(3), 26.258(4)	14.683(5)	15.677(2)
α, deg			92.23(1)
β, deg	90.72(1), 90.45(1), 90.32(1)	94.02(2)	94.79(1)
γ, deg			94.79(1)
V, $Å^3$	5560.7(7), 5679(1), 5729(1)	2080.7(12)	1503.3(4)
ρ_{calcd}, g cm^{-3}	1.181 1.146	1.734	1.529
R^a	0.0512, 0.0587	0.070	0.073
R_w [b]	0.119, 0.155	0.177	0.178

[a] $R(F) = \sum||F_o| - |F_c||/\sum|F_o|$. [b] $R_w = (\sum[w(F_o^2 - F_c^2)^2]/\sum[wF_o^2)^2])^{1/2}$, $[I > 2\sigma(I)]$.

Table 2. Selected Bond Distances (Å) and Angles (deg) for **1**-BPh_4 and Torsional Angles of the NCH_2CH_2N Chelate Rings of Me_3tacn at −30 and 90 °C

	−30 °C	90 °C
Fe−N(1)	2.049(3)	2.142(5)
Fe−N(2)	2.059(3)	2.150(4)
Fe−N(3)	2.054(3)	2.141(5)
Fe−N(4)	1.959(4)	2.085(5)
Fe−N(5)	1.971(4)	2.107(6)
Fe−N(6)	1.996(4)	2.138(5)
	−30 °C	90 °C
N(1)−Fe−N(2)	84.38(14)	82.4(2)
N(1)−Fe−N(3)	85.1(2)	83.4(2)
N(2)−Fe−N(3)	84.8(2)	82.5(2)
N(4)−Fe−N(5)	90.1(2)	90.2(2)
N(4)−Fe−N(6)	91.58(13)	92.0(2)
N(5)−Fe−N(6)	86.80(13)	86.4(2)
N(1)−Fe−N(4)	92.5(2)	93.5(2)
N(1)−Fe−N(6)	94.81(14)	96.1(2)
N(2)−Fe−N(4)	91.70(14)	92.7(2)
N(2)−Fe−N(5)	93.86(14)	94.9(2)
N(3)−Fe−N(5)	92.2(2)	92.7(2)
N(3)−Fe−N(6)	91.9(2)	92.8(2)
N(1)−Fe−N(5)	176.9(2)	175.5(2)
N(3)−Fe−N(4)	175.9(2)	174.5(2)
N(2)−Fe−N(6)	176.65(14)	175.2(2)
	−30 °C	90 °C
N(1)−C(1)−C(2)−N(2)	24.8(8)	32(1)
N(2)−C(3)−C(4)−N(3)	23.8(9)	35(1)
N(3)−C(5)−C(6)−N(1)	22(1)	28(2)

Table 3. Selected Bond Distances (Å), Bond Angles (deg), and Torsional Angles of the NCH_2CH_2N Chelate Rings of Me_3Tacn in **3** and **4**

3		**4**	
Fe−N(1)	2.196(6)	Fe−N(1)	2.214(5)
Fe−N(2)	2.216(5)	Fe−N(2)	2.208(5)
Fe−N(3)	2.200(6)	Fe−N(3)	2.180(5)
Fe−N(4)	2.145(6)	Fe−O(1)	2.137(4)
Fe−N(5)	2.143(6)	Fe−O(4)	2.142(4)
Fe−O(1)	2.081(5)	Fe−O(7)	2.070(5)
3		**4**	
N(1)−Fe−N(2)	80.7(2)	N(1)−Fe−N(2)	80.5(2)
N(1)−Fe−N(3)	81.3(2)	N(1)−Fe−N(3)	81.0(2)
N(2)−Fe−N(3)	80.3(2)	N(2)−Fe−N(3)	81.1(2)
N(4)−Fe−N(5)	90.3(2)	O(1)−Fe−O(4)	89.6(2)
N(4)−Fe−O(1)	92.3(2)	O(1)−Fe−O(7)	92.4(2)
N(5)−Fe−O(1)	91.4(2)	O(4)−Fe−O(7)	89.9(2)
N(1)−Fe−N(4)	94.7(2)	N(1)−Fe−O(4)	93.3(2)
N(1)−Fe−N(5)	93.3(2)	N(1)−Fe−O(7)	93.4(2)
N(2)−Fe−O(1)	91.9(2)	N(2)−Fe−O(1)	95.9(2)
N(2)−Fe−N(5)	95.0(2)	N(2)−Fe−O(7)	97.8(3)
N(3)−Fe−N(4)	94.0(2)	N(3)−Fe−O(1)	93.2(2)
N(3)−Fe−O(1)	93.5(2)	N(3)−Fe−O(4)	90.7(2)
N(3)−Fe−N(5)	173.3(2)	N(1)−Fe−O(1)	173.6(2)
N(2)−Fe−N(4)	173.2(2)	N(2)−Fe−O(4)	170.4(2)
N(1)−Fe− O(1)	171.5(2)	N(3)−Fe−O(7)	174.4(2)
3		**4**	
N(1)−C(1)−C(2)−N(2)	−48.7(8)	N(1)−C(1)−C(2)−N(2)	32(1)
N(2)−C(3)−C(4)−N(3)	−49.0(9)	N(2)−C(3)−C(4)−N(3)	35(1)
N(3)−C(5)−C(6)−N(1)	−49.5(9)	N(3)−C(5)−C(6)−N(1)	28(1)

anion, but as we show in this report, triflate will bind to iron(II) in competition with solvent molecules or other Lewis bases. In those cases where we do not want a coordinated anion, we utilize tetraphenylborate salts. The synthetic reactions presented in this paper are summarized in Scheme 1. Reactions of $Fe(OTf)_2$ with Me_3tacn in acetone, DMF, DMSO, or methanol afford very air-sensitive solutions that are colorless. However, in acetonitrile an equimolar ratio of $Fe(OTf)_2$ and Me_3tacn affords a purple solution from which the LS complex $[Fe(Me_3tacn)(CH_3CN)_3](OTf)_2$ (**1**−OTf) can be crystallized by addition of diethyl ether (eq 1). The presence of the three terminal acetonitrile ligands was confirmed from IR spectra (2270, 2298 nm). Complex **1**−OTf loses its acetonitrile ligands when dried under a vacuum, or even under dinitrogen at 1 atm, to afford a colorless solid that analyzes as $Fe(Me_3tacn)(OTf)_2$ (**2**). Purple crystals are formed within a few minutes on the addition of $NaBPh_4$ to acetonitrile solutions of **1**−OTf. These crystals are stable to loss of bound acetonitrile molecules even under a vacuum and analyze as $[Fe(Me_3tacn)(CH_3CN)_3](BPh_4)_2$ (**1**−BPh_4). An X-ray crystal structure study of this complex confirms the presence of the bound acetonitrile ligands.

The reaction of $Fe(OTf)_2$ with 2.0 equiv of Me_3tacn in CH_2Cl_2 followed by layering pentane on the solution affords a few purple crystals of **1**−OTf and some large colorless crystals that have been shown by X-ray crystallography to be $[Fe(Me_3tacn)(MeCN)_2(OTf)](OTf)\cdot CH_2Cl_2$ (**3**$\cdot CH_2Cl_2$). These crystals are unstable to loss of acetonitrile and could not be characterized by other techniques. However, NMR spectroscopy described below provides evidence that **3**, or a complex with similar symmetry, exists in solution. All attempts to obtain crystals of

(23) Goedkin, V. L.; Merrell, P. H.; Busch, D. H. *J. Am. Chem. Soc.* **1972**, *94*, 3397−3405.

Scheme 1

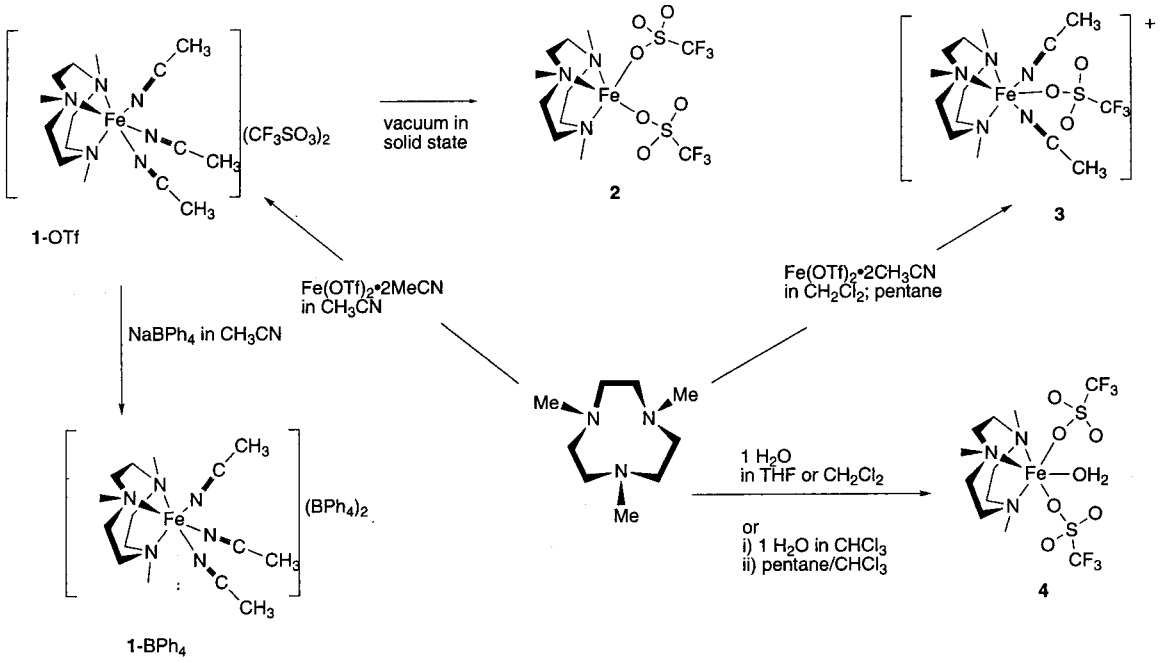

2 that are suitable for a crystal structure determination have failed. Very fragile thin plates were obtained by layering heptane on CH_2Cl_2 solutions of **2**.

A colorless solution is formed when **1**−OTf is dissolved in noncoordinating solvents such as methylene chloride or chloroform, or in oxygen donor solvents such as acetone, THF, DMSO, or DMF. When **1**−OTf is dissolved in methylene chloride at room temperature, a colorless solution forms and the remaining undissolved solid loses its color. When cold (less than −15 °C) methylene chloride is added to solid **1**−OTf, a transient purple solution forms that is rapidly bleached, reflecting the facile loss of coordinated acetonitrile. The presence of 1 equiv of water in THF or CH_2Cl_2 affords colorless crystals of $Fe(Me_3tacn)(H_2O)(OTf)_2$ (**4**) in which both triflate anions and the water molecule are coordinated. The BPh_4 salt of **1** is sparingly soluble in noncoordinating solvents but affords colorless solutions in DMF, DMSO, and acetone. This suggests that it is the triflate anions or coordinating solvents that facilitate the loss of coordinated acetonitrile.

Crystal Structures of Iron(II) Complexes. A summary of crystal data for **1**−BPh_4, **3**, and **4** are collected in Table 1, and selected bond distances and angles are presented in Table 2. Complex **1**, presented in Figure 1, is well separated from the two BPh_4 anions. The iron resides in a distorted N_6 environment, three nitrogens from the facially coordinating Me_3tacn ligand and the other three from acetonitrile molecules. There is no crystallographically imposed symmetry on **1**, although it approaches C_3 point symmetry. There is a pucker in the five-membered $FeNCH_2CH_2N$ chelate rings, but the constraints of the macrocycle limit it to be much less dramatic than observed in ethylenediamine complexes. The carbon atoms are all on the same side of the NFeN planes with an average deviation of 0.28(5) Å for C1, C3, and C5 and 0.53(4) Å for C2, C4, and C6 from the respective NFeN planes. This contrasts with the pucker of ethylenediamine complexes such as $[Fe(en)_3](OTf)_2$,[24] where the carbon atoms lie on opposite sides of the NFeN planes (by −0.30 and 0.42 Å, and the average N−C−C−N torsional angles is 58°). The three NCH_2CH_2N fragments of the ligand adopt either the $\delta\delta\delta$ or $\lambda\lambda\lambda$ configurations, and the centrosymmetric space group of **1**−BPh_4 requires the presence of a racemic mixture of complexes in the crystal. The relatively large anisotropic thermal parameters of the methylene carbons indicate the presence of either a dynamic or static disorder in the degree of pucker of the ring. This disorder is reflected in apparently shorter than normal N−C and C−C bonds within the macrocycle.

Distortions from octahedral symmetry for the FeN_6 unit are most apparent in the N_{amine}−Fe−N_{amine} angles that are enforced to be less than 90° (ave 84.8°) by the five-membered rings within the chelate ligand. The average values of the three unconstrained $N_{nitrile}$−Fe−$N_{nitrile}$ angles is 89.5°, of the six *cis*−$N_{nitrile}$−Fe−N_{amine} angles is 92.8°, while that of the trans angles is 176.5°. The Fe−N_{amine} bonds (ave 2.054(4) Å) are significantly longer than the Fe−$N_{nitrile}$ bonds (ave 1.98(2) Å). The

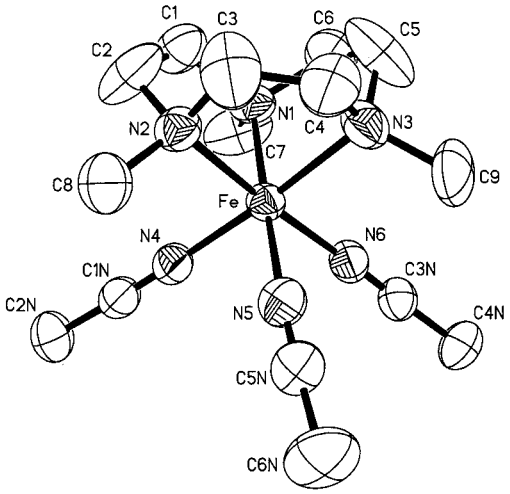

Figure 1. Molecular structure and atom labeling scheme for $[Fe(Me_3tacn)(MeCN)_3](BPh_4)_2$ (**1**−BPh_4). All hydrogen atoms have been omitted for clarity. Thermal ellipsoids are at the 30% probability level.

(24) (a) On $[Fe(en)_3](OTf)_2$. Nair, V. S. Ph.D. Thesis, Emory University, Atlanta, GA, 1996. (b) On $[Fe(en)_3]_2(Hg_2Te_9)$. Li, J.; Rafferty, B. G.; Mulley, S.; Proserpio, D. M. *Inorg. Chem.* **1995**, *34*, 6417−6418. (c) On $[Fe(en)_3]_n(In_2Te_6)_n$. Li, J.; Chen, Z.; Emge, T. J.; Proserpio, D. M. *Inorg. Chem.* **1997**, *36*, 1437−1442.

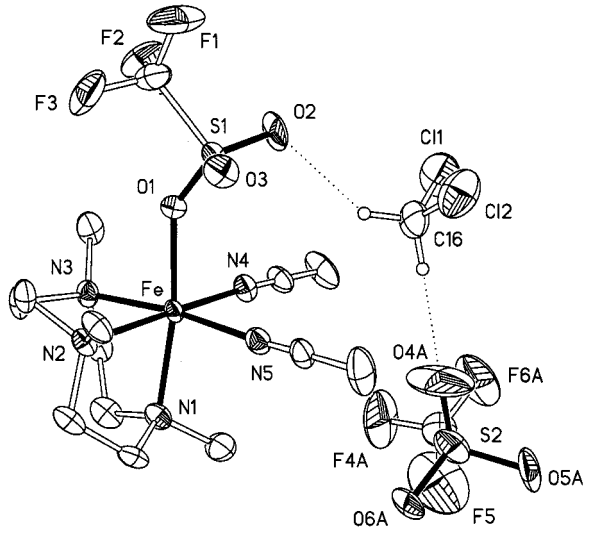

Figure 2. Molecular structure and atom labeling scheme for [Fe(Me_3-tacn)$(MeCN)_2$(OTf)](OTf)·CH_2Cl_2 (**3**) illustrating the intermolecular hydrogen-bonding interactions. All hydrogen atoms except on the CH_2Cl_2 have been omitted for clarity. Thermal ellipsoids are at the 30% probability level.

analogous complex with the unhindered ligand tacn, [Fe(tacn)$(MeCN)_3]^{2+}$,[3] has slightly shorter bonds (Fe−N_{amine} 1.998(8) Å and Fe−$N_{nitrile}$ 1.943(8) Å), but the sandwich complex, [Fe$(tacn)_2]^{2+}$,[2,3] has similar Fe−N_{amine} bonds (ave 2.032(6) Å). These bond lengths in this purple complex are typical of LS iron(II) amine bonds. The short bonds result in a tighter fit of the smaller LS Fe within the tridentate macrocycle. The Fe lies only 1.289(2) Å above the plane of the three amine nitrogen atoms.

Heating the crystal to 90 °C from −30 °C causes the average Fe−N_{amine} bond lengths to increase by 0.090 Å or 4% to 2.144 Å. The Fe−$N_{nitrile}$ bond lengths increase by 0.135 Å or 6.8% to 2.110 Å, and the iron moves out to the plane of the three amine nitrogens by almost 0.1 Å to 1.386(2) Å. Magnetism data described below indicate that the sample needs to be above at least 150 °C before it is completely in the HS form.

The iron(II) exists in the HS state in **3**, in which one of the acetonitrile ligands is replaced by a triflate. The average Fe−N_{amine} bond lengths increase to 2.204 Å and the average Fe−$N_{nitrile}$ bonds increase to 2.144 Å, which results in the iron atom being 1.462(3) Å above the plane of the three amine nitrogens. This complex is depicted in Figure 2, and selected metrical parameters are collected in Table 3. The FeN_5O coordination sphere of the iron has approximate C_s symmetry. The coordinated triflate forms a relatively strong hydrogen bond to a CH_2Cl_2 solvate molecule (C(16)···O(2) 3.20 Å, C−H···O(2) 2.27 Å, and C−H···O 143°).[25] This solvent molecule forms a bridge to the triflate counterion (C(16)···O(4a) 3.13 Å, C−H···O(2) 2.08 Å, and C−H···O 163°). The Fe−OTf bond is shorter in this cationic complex than in the neutral *trans*-Fe$(MeCN)_4(OTf)_2$,[22] or in **4** described below.

Replacing the three acetonitrile ligands of **1** by two triflates and a water results in the neutral complex **4** (Figure 3 and Table 3). The coordinated water ligand forms hydrogen bonds to oxygens of two triflates of an adjacent molecule related to the first by an inversion center as indicated by the O7···O2′ and O7···O6′ distances of 2.744(9) and 2.720(8) Å, respectively.

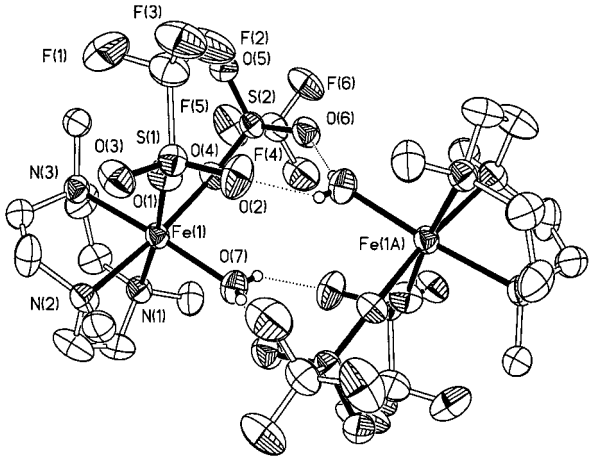

Figure 3. Molecular structure and atom labeling scheme for {Fe(Me_3-tacn)$(H_2O)(OTf)_2\}_2$ (**4**) illustrating the intermolecular hydrogen-bonded pair of molecules. All hydrogen atoms except on the H_2O have been omitted for clarity. Thermal ellipsoids are at the 30% probability level.

The centrosymmetric binuclear iron complex, in which the Fe···Fe distance is 6.123(2) Å, is held together by four hydrogen bonds between the two aqua ligands and coordinated triflates. The metrical parameters of this colorless complex are typical of HS iron(II) and are very similar to the analogous iron(II)[26] and copper(II)[27] complexes with the bulkier ligand *i*-Pr_3tacn. The Fe−N_{amine} bonds (ave 2.20(2) Å) are longer than in **1**, and the distance of the Fe to the plane of the amine nitrogens (1.458(3) Å) is considerably further than in **1** but almost the same as in **3**. The triflates adopt a bridging mode between the iron and aqua ligands, which causes a lengthening of the iron to triflate bonds (Fe−O(1) 2.137(4) Å and Fe−O(4) 2.142(4) Å) that are longer than in **3**. The bond to the water (Fe−O(7) 2.070(5) Å) is shorter than in $[Fe(H_2O)_6](OTf)_2$ (2.103(3) Å), where the aqua ligands are involved in extensive hydrogen bonding to uncoordinated triflates.[22]

Electronic Spectroscopy. The intense purple color of **1** observed in the solid is also seen in acetonitrile solutions. There is a marked temperature dependence of the intensities of the absorption maxima at 389, 560, and 880 nm. The two highest energy bands are typical of octahedral LS iron(II), with d−d bands corresponding to the $^1A_{1g} \rightarrow {}^1T_{1g}$ and $^1A_{1g} \rightarrow {}^1T_{2g}$ spin-allowed transitions, and the near-IR band is assigned to the $^5T_{2g} \rightarrow {}^5E_g$ transition of the HS complex. The energies of d−d bands of the LS complex are almost identical to those of the *trans*-[Fe$(Me_6[14]aneN_4)(MeCN)_2]^{2+}$ complex,[19] and at higher energy than the complexes coordinated solely by multidentate aliphatic amines, [Fe(*trans*-diammac)$]^{2+}$ (405 and 584 nm),[28] [Fe$(tacn)_2]^{2+}$ (387 and 601 nm),[2] and [Fe$((NH_2)_2sar)_2]^{2+}$ (394 and 590 nm). The intensities of the visible bands of **1** increase on lowering the temperature, while the intensities of the near-IR band decrease as the temperature is lowered (Figure 4). The d−d bands of **1**−BPh_4 in acetonitrile solutions are more intense than those of **1**−OTf, which is consistent with the NMR studies that indicate that there should be more LS complex in the absence of triflate. Complete conversion to the LS form does not occur in the temperature range accessible with acetonitrile or butyronitrile solutions.

(25) (a) Desiraju, G. R. *Acc. Chem. Res.* **1991**, *24*, 290−296. (b) Desiraju, G. R. *Acc. Chem. Res.* **1996**, *29*, 441−449. (c) Steiner, T.; Desiraju, G. R. *J. Chem. Soc., Chem. Commun* **1998**, 891−892.

(26) Diebold, A.; Hagen, K. S. *Inorg. Chem.*, submitted.

(27) Halfen, J. A.; Mahapatra, S.; Wilkinson, E. C.; Gengenbach, A. J.; Young, V. G., Jr.; Que, L., Jr.; Tolman, W. B. *J. Am. Chem. Soc.* **1996**, *118*, 763−776.

(28) Börzel, H.; Comba, P.; Pritzkow, H.; Sickmüller, A. F. *Inorg. Chem.* **1998**, *37*, 3853−3857.

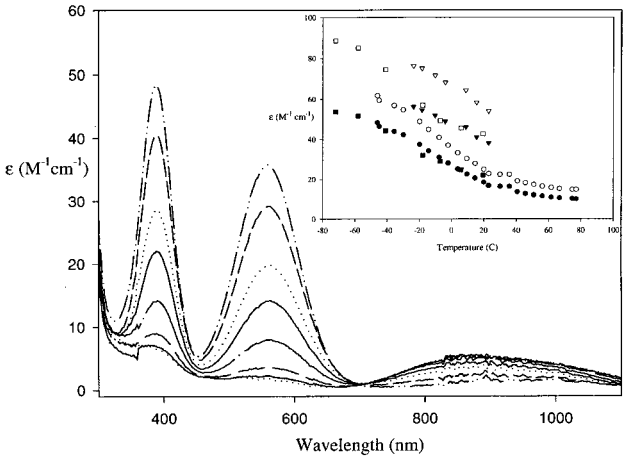

Figure 4. Variable temperature UV−vis−NIR spectra of [Fe(Me_3tacn)(MeCN)$_3$](OTf)$_2$ in MeCN from −46 to 77 °C. Inset: plot of extinction coefficient vs temperature for **1**−OTf (■ 562 nm, □ 388 nm) and **1**−BPh_4 in MeCN (▲ 557 nm, △ 384 nm) and **1**−OTf in PrCN (○ 560 nm, ● 382 nm).

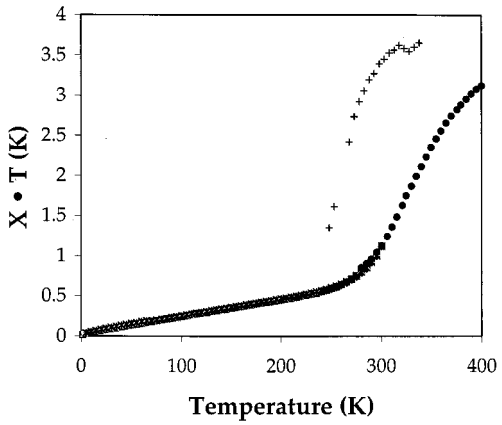

Figure 5. Variable temperature SQUID magnetic susceptibility data on a solid sample of **1**−BPh4, and MeCN solution data on **1**−OTf (+) by Evans' method.

Magnetism in Solid State and in Solution. The purple complex **1**−BPh_4 exhibits a magnetic moment of 2.4 μ_B in the solid state at room temperature that is indicative of a spin-crossover system.[29] A variable temperature study of the magnetism of **1**−BPh_4 (Figure 5) shows that the magnetic moment gradually increases from ~0.5 μ_B below 2 K to 2.4 μ_B at room temperature and subsequently increases more rapidly until it begins to level off at about 5.3 μ_B above 400 K. This gradual transition is not unusual for iron(II) complexes that undergo a spin transition.[4−10] However, a purple solid sample of **1**−OTf has a magnetic moment of 3.5 μ_B that increases to a value of 5.4 μ_B, typical of HS iron(II), when the sample is placed in a vacuum. The color is lost and a weight loss of 16.9%, corresponding to loss of 2.7 acetonitrile molecules, occurs at the same time. The initial high value is a consequence of the difficulty in obtaining a dry sample of **1**−OTf that has not lost any of its coordinated acetonitrile. In CD_2Cl_2 solution, the room-temperature magnetic moment of **2** is 5.7 μ_B. However, the magnetic moment of **1**−OTf in CD_3CN decreases from 5.4 μ_B at 338 K to 3.3 μ_B at 248 K (Figure 5). At a given temperature, the solution state magnetic moment is considerably higher than that in the solid state. Clearly, the ligand field strength is weaker in solution, caused by a weaker binding of the ligands in solution, a net drop in coordination number caused by rapid exchange of coordination MeCN, or displacement of coordinated MeCN by triflate. Similar behavior is observed when iron(II) is encapsulated in a macrobicyclic ligand as in [Fe($(NH_2)_2$-sar)]$^{2+}$ [20] or sandwiched between tridentate ligands as in [Fe($tacn)_2$].[30] The triflate salts of these complexes are diamagnetic in the solid state but are paramagnetic in solution. Even in the solid state the magnetism of these complexes is sensitive to the crystal lattice. Polycrystalline samples of [Fe($tacn)_2$]Br_2·$4H_2O$ are diamagnetic in the solid state but become paramagnetic when the water of crystallization is removed under vacuum.[31] The solution behavior of iron(II) complexes of Me_3tacn is better addressed by NMR spectroscopy from which the number and symmetry of species in solution can be inferred.

Solution Behavior According to ^{1}H, ^{2}H, and ^{19}F NMR. Analysis of stereochemistry and detection and characterization of the structural and electronic equilibria that occur in solutions of these complexes are effectively monitored by a combination of ^{1}H, ^{2}H, and ^{19}F NMR spectroscopy.[16,18,26,32] The multiple equilibria that can exist in solution are summarized in Scheme 2. The spectrum of the purple solution of **1**−BPh_4 exhibits the expected phenyl resonances of the anion, but the rest of the spectrum is characteristic of isotropicaly shifted resonances of a paramagnetic complex. Only three resonances are seen at 81.7, 50.9, and 29.6 ppm downfield of TMS at room temperature with relative intensities of 2:3:2.

On the basis of symmetry, **1** should consist of an equal mixture of enantiomers that have approximate C_3 point symmetry in the solid state. In this arrangement, four resonances should be observed in the spectrum for the three equivalent NCH_2CH_2 fragments of the ligand, one for the equivalent methyl groups of the ligand, and an additional resonance for the three equivalent methyl groups of the acetonitrile ligands. The four distinct methylene protons under C_3 symmetry fall into two groups, H-syn and H-anti relative to the Fe atom. There are axial and equatorial orientations in each of these groups, H-syn$_{ax}$, H-syn$_{eq}$, H-anti$_{ax}$, and H-anti$_{eq}$. A simple twist of the NCH_2-CH_2N groups interconverts the $\lambda\lambda\lambda$ and $\delta\delta\delta$ isomers and transforms the environments of H-anti$_{ax}$ ↔ H-anti$_{eq}$ and H-syn$_{ax}$ ↔ H-syn$_{eq}$. The observation of three isotropically shifted resonances is a consequence of this dynamic exchange between the axial and equatorial methylene positions in the chelate rings of **1**. The CH_3CN resonances are not observed because of exchange with bulk CD_3CN. The isotropically shifted resonances are consistent with a species with time-averaged C_{3v} symmetry corresponding to the twist described above that interconverts the $\lambda\lambda\lambda$ and $\delta\delta\delta$ isomers rapidly on the time scale of the NMR experiment. Thus, only two resonances are observed for the unique CH_2 protons in addition to the one resonance for the CH_3 protons.

The room-temperature spectrum of the colorless solution of **1**−BPh_4 in DMSO-d_6 also exhibits three isotropically shifted ^{1}H resonances, but these are further downfield-shifted at 115.9, 79.5, and 41.3 ppm with the same relative intensities of 2:3:2 as seen in CD_3CN. A broad feature centered at 2 ppm is due to the acetonitrile ligands displaced by bulk solvent. This is confirmed in the ^{2}H NMR spectrum of [Fe(Me_3tacn)$_3$(CD_3CN)$_3$]-(BPh_4)$_2$ in DMSO in which a relatively sharp resonance is seen

(29) Figgis, B. N. *Introduction to Ligand Fields*; Wiley-Interscience: New York, 1966.
(30) Wieghardt, K.; Schmidt, W.; Herrmann, W.; Küppers, H. J. *Inorg. Chem.* **1983**, *22*, 2953−2956.
(31) Wieghardt, K.; Küppers, H. J.; Weiss, J. *Inorg. Chem.* **1985**, *24*, 3067.
(32) Holm, R. H.; Hawkins, C. J. In *NMR of Paramagnetic Molecules*; LaMar, G. N., Horrocks, W. D., Holm, R. H., Eds.; Academic Press Inc.: New York, 1973; Chapter 7.

Scheme 2. Solution Dynamics by NMR

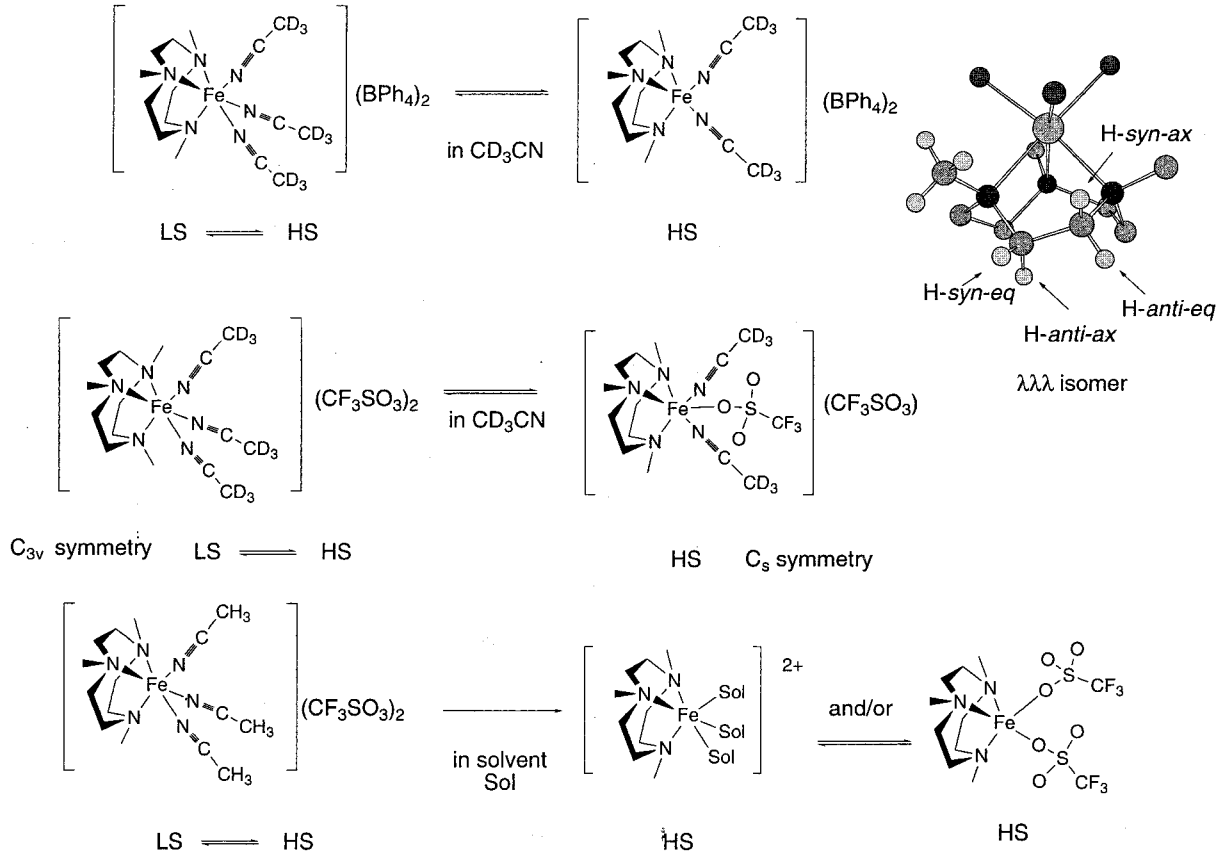

at 1.8 ppm. The spectrum of **1**−OTF in CD_2Cl_2 is similar to that of **1**−BPh_4 in DMSO-d_6 except that the three shifted ^{1}H resonances occur at 131, 104.5, and 50.1 ppm at room temperature. The difference in shifts is still consistent with HS iron(II) but with a different structure than in DMSO solution. This can be verified by an analysis of the ^{19}F NMR spectra. The triflates should be coordinated to the HS iron(II) center in CD_2Cl_2, but DMSO is a coordinating solvent and displaces both the acetonitrile molecules and the triflates. Only one sharp ^{19}F resonance is seen at −76.8 ppm in solutions of **1** in DMSO-d_6, which is consistent with uncoordinated triflate experiencing little or no isotropic shift induced by the paramagnetic complex. However, the behavior of **1**−OTF and **2** in CD_2Cl_2 is more complicated. While two broad ^{19}F resonances are observed at −12.1 and −77.3 ppm for **1**−OTf in CD_3CN, three broad resonances are seen at 60.4, −14.0, and −69.7 ppm in CD_2Cl_2 at room temperature (Figure 10e). Three ^{19}F resonances are seen at 59, −15, and −64 ppm at room temperature when **2**, which has no coordinated MeCN, is dissolved in CD_2Cl_2. Clearly, the triflates are involved in the coordination sphere of the iron in these solvents.

Variable Temperature Solution Behavior in Coordinating Nitrile Solvents. At room temperature, the ^{1}H NMR spectrum of **1**−OTf in CD_3CN exhibits four broad but clearly defined resonances at 97, 83, 52, and 31 ppm with two smaller broad resonances at 115 and 62. Clearly, one or more species with time-averaged symmetry lower than C_{3v} exists in CD_3CN solutions of **1**−OTf. An equilibrium exists in solution between species having different structures that interconvert slowly on the time scale of the experiment. Identification of these species requires an analysis of the temperature dependence of the resonances of the Me_3tacn ligand as well as the triflate anion. Spectral assignments of resonances for the complexes in solution are simplified by the use of the selectively deuterated ligand, $(CD_3)_3$tacn, and a combination of both ^{1}H and ^{2}H NMR.

We first analyze the variable temperature behavior of **1**−BPh_4 where there should be no interference from the anion. The temperature dependence of the shifted ^{1}H resonances of **1**−BPh_4 in CD_3CN is plotted in Figure 6. Large shifts at high temperature that decrease to near-diamagnetic values at low temperature are indicative of the non-Curie behavior expected of a LS ↔ HS process. The temperature range accessible for these NMR experiments covers almost the entire transition from LS to HS. In spectra of iron(II) encapsulated within macrobicyclic ligands as in $[Fe(sar)]^{2+}$ and $[Fe((NH_2)_2sar)]^{2+}$,[20] or sandwiched between two tridentate ligands as in $[Fe(tacn)_2]^{2+}$ [3] and $FeTp_2$,[33] a non-Curie relationship between shifts and temperature was also observed. However, the leveling off in shifts at the maximum

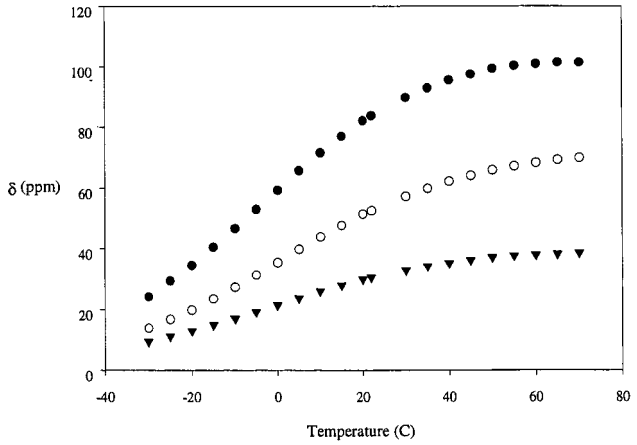

Figure 6. Plot of variation of chemical shifts of ^{1}H NMR resonances of **1**−BPh_4 in CD_3CN with temperature.

that would be expected for complete conversion to the HS form or complete conversion to the LS form was not observed in the accessible temperature range of the NMR experiments carried out. This contrasts with the behavior of the isotropically shifted resonances of **1**−BPh_4 in CD_3CN (Figure 6 and Table S1 in Supporting Information). The shifts almost level off at both the low- and high-temperature extremes of the 100 °C temperature range accessible in CD_3CN. The leveling off at high temperature may be indicative of the involvement of more than one equilibrium process occurring in solution. One process is the conventional LS ↔ HS crossover between $^1A_1$ and $^5T_2$ electronic configurations typical of an intermediate strength ligand field. An additional LS ↔ HS equilibrium could exist between the six-coordinate **1** and another HS species of lower coordination number formed by dissociation of bound acetonitrile (see Scheme 2). Both of these equilibration processes are fast on the time scale of the experiment, and the averaged spectra of all equilibrated species are observed. The facile loss of bound acetonitrile is evident from the spectra in other solvents, and it is only in coordinating nitrile solvents, where there exists a large excess of solvent, that the equilibrium involves **1**. Larger shifts that are typical of HS complexes and that generally decrease with increasing temperature, as expected for Curie behavior, are observed in other solvents.

The methyl substituents enhance the lability of the coordinated acetonitrile ligands. The leveling off of isotropic shifts at higher temperatures does not occur in $[Fe(tacn)(MeCN)_3](BPh_4)_2$, which incorporates the unsubstituted ligand tacn.[3] Bulkier substituents, *i*-Pr and *i*-Bu, prevent LS complexes from forming, and the former enforces five-coordinate complexes with Co(II) and Fe(II).[26] Similar behavior has been observed with the tetradentate tripodal ligand, tpa, in $[Fe(tpa)(MeCN)_2]^{2+}$ [18] and it's methyl-substituted derivatives 6-Metpa, 6-Me_2tpa, and 6-Me_3tpa.[34] The unsubstituted tpa complexes exhibit C_{3v} symmetry in solution, which requires ligand substitution that is rapid on the NMR time scale even for the LS complexes. These methyl-substituted ligands form HS complexes at room temperature, although no variable temperature studies were reported. However, it is well established that methyl substitution can convert LS iron(II) complexes to HS complexes.[35]

The greater number of resonances observed in the spectra of **1**−OTf in acetonitrile (Figure 7c and Table S2 in Supporting Information) than what occurs with **1**−BPh_4 described above is a result of multiple equilibria that are made more complicated by the presence of the triflate ion. In addition to the LS ↔ HS crossover of the C_{3v} complex **1**, a second equilibrium probably involves a species with a structure similar to **3**, obtained when a triflate displaces a bound acetonitrile (Scheme 2). With the ligand $(CD_3)_3$tacn, only one set of three relatively sharp resonances (two in the ^1H and one in the ^2H spectra) are observed above 50 °C (Figure 8). The isotropic shifts are nearly temperature-independent above this temperature, indicating that all species are HS and in rapid equilibrium. As the temperature is lowered below 45 °C, the methyl resonance broadens and splits into two resonances that are upfield and downfield relative to the 70 °C spectrum (Figure 7e and open and filled circles in Figure 8b). The two methylene resonances also split into two sets of resonances below this temperature. One relatively sharp set shifts upfield with decreasing temperature, which is consistent with a HS species (Figure 7d at 35 °C and closed and open triangles between 45 and 25 °C in Figure 8a). The second set shifts downfield, which is consistent with a spin-crossover

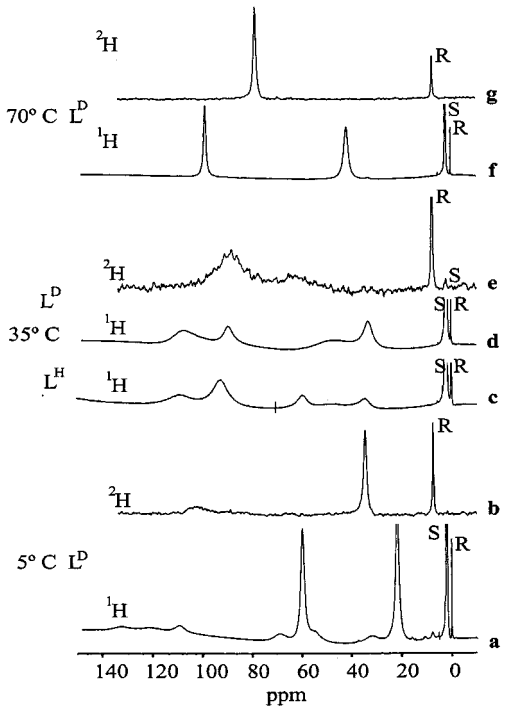

Figure 7. ^1H and ^2H NMR spectra of $[Fe(L)(MeCN)_3](OTf)_2$ (L^H = $(CH_3)_3$tacn or L^D = $(CD_3)_3$tacn in CD_3CN for ^1H NMR at 500 MHz and in CH_3CN for ^2H NMR at 92 MHz.

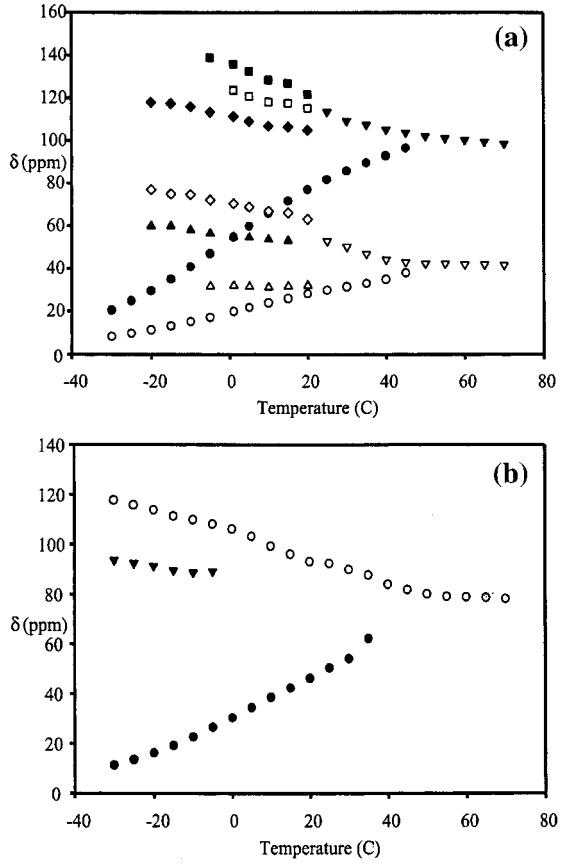

Figure 8. Plot of variation of chemical shifts of resonances of $[Fe((CD_3)_3tacn)(MeCN)_3](OTf)_2$ with temperature corresponding to spectra of Figure 7: (a) ^1H NMR resonances in CD_3CN; (b) ^2H NMR resonances of **1**−OTf in CH_3CN.

(33) Jesson, J. P.; Trofimenko, S.; Eaton, D. R. *J. Am. Chem. Soc.* **1967**, *89*, 3158−3164.
(34) Zang, Y.; Kim, J.; Dong, Y. H.; Wilkinson, E. C.; Appelman, E. H.; Que, L., Jr. *J. Am. Chem. Soc.* **1997**, *119*, 4197−4205.
(35) Nelson, S. M.; Rodgers, J. *J. Chem. Soc. A* **1968**, 272−276.

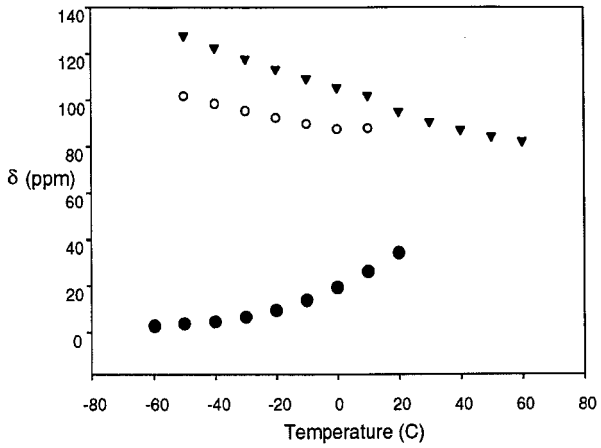

Figure 9. Plot of variation of chemical shifts of ^{2}H NMR resonances of $[Fe((CD_3)_3tacn)(PrCN)_3])(OTf)_2$ in $CH_3CH_2CH_2CN$ (PrCN) with temperature.

species (Figure 7d and closed and open circles in Figure 8a). The resonances are broad because the system is just below the coalescence temperature and the exchange process between two species is comparable to the time scale of the experiment. Both species have time-averaged C_{3v} symmetry in this temperature range. As the temperature is lowered below 20 °C to −10 °C, the HS species exhibits six resonances that are consistent with a C_s symmetry species such as **3**. The 5 °C spectrum is shown in Figure 7a where the six resonances are shifted further than the corresponding six resonances observed in the time-averaged C_{2v} symmetry complex $[Fe_2(OH)(Ph_3CCOO)_2((CD_3)_3tacn)_2]^+$.[36] As can be seen in spectra a and b of Figure 7, the relative intensities of the HS species are very low, and below −10 °C they are barely discernible from the baseline.

The ^{19}F NMR spectra of **1**−OTf in acetonitrile support this interpretation. The two broad resonances that are observed in the CD_3CN solution at −12.1 and −77.3 ppm at room temperature broaden and shift to −15.7 and −76.7 ppm on warming the solution to 50 °C. The same resonances sharpen and appear at −0.5 and −77.6 ppm at −25 °C. The intensity of the downfield resonance decreases to almost nothing at the lowest temperatures. The downfield resonance is consistent with a triflate terminally coordinated in a HS complex such as **3**. Not only does the LS form of spin-crossover species **1**−OTf predominate at the lowest temperatures, but it is favored over HS species such as **3**.

To favor the existence of the HS complex at low temperature, we studied the ^{2}H spectra in butyronitrile (PrCN). It was anticipated that the greater bulk of butyronitrile would prevent complete conversion to the LS complex $[Fe(Me_3tacn)(PrCN)_3](OTf)_2$ (**1**−PrCN) at low temperature and would allow a HS species such as $[Fe(Me_3tacn)(PrCN)_2(OTf)](OTf)$ (**3**−PrCN) to form. The temperature dependence of the ^{2}H shifts of the resonances is plotted in Figure 9 and compiled in Table S3. Three resonances that correspond to two different complexes are seen over the temperature range 20 to −50 °C (Figure S4 of Supporting Information). The downfield resonances at 109 and 89 ppm at −10 °C have a 2:1 ratio of integrated intensities, which is consistent with a species of C_s symmetry such as **3**−PrCN. The upfield resonance at 14 ppm is sharper than the other two and is consistent with the structure of **1**−PrCN with time-averaged C_{3v} symmetry. As the temperature is lowered, the resonances of **3**−PrCN shift further downfield as is expected

(36) Payne, S. C.; Hagen, K. S. Manuscript submitted for publication.

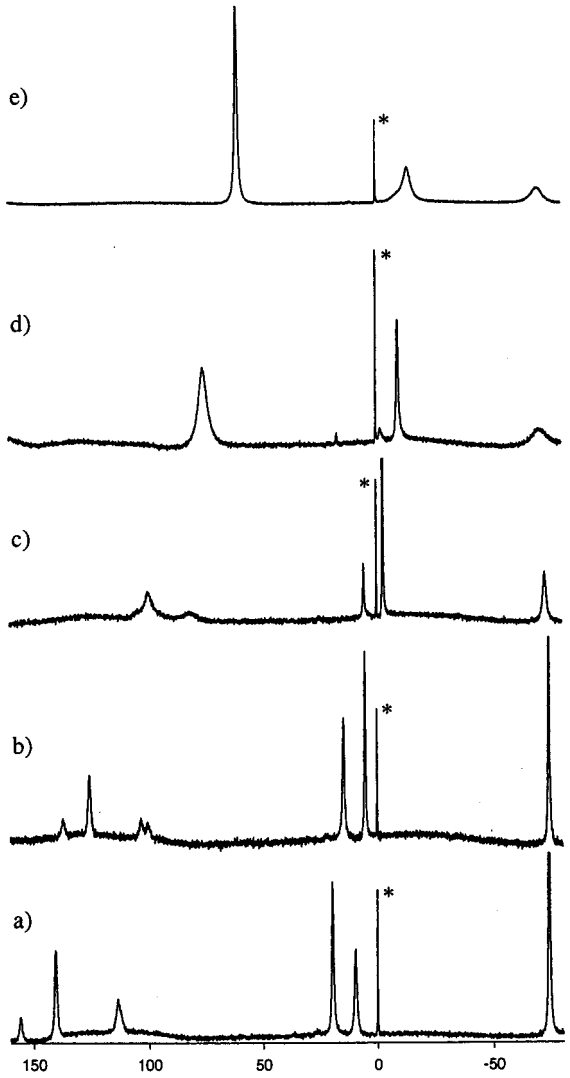

Figure 10. Variable temperature ^{19}F NMR of $[Fe(Me_3tacn)(MeCN)_3](OTf)_2$ in CD_2Cl_2 at 282 MHz. Spectra were acquired at the following temperatures: (a) −80 °C, (b) −65 °C, (c) −35 °C, (d) −5 °C, and (e) 25 °C.

for a HS complex and decrease in intensity until at −60 °C they are no longer discernible from the baseline. Only one resonance at 2.7 ppm is seen at this temperature, which is consistent with almost complete conversion to the LS complex. As the temperature is raised, the two resonances of **3**−PrCN broaden and coalesce above 10 °C and the intensity of the single resonance of **1**−PrCN decreases until it is not seen at and above 30 °C. The single remaining resonance sharpens because of rapid exchange of ligands on the remaining HS complex(es). This interpretation is also supported by the room temperature ^{19}F NMR spectra where separate resonances for bound triflates (as in **3**−PrCN) and free triflates (as in **3**−PrCN) are seen at −5.9 and −76.5 ppm, respectively.

Solution Behavior in Noncoordinating Solvents. The room temperature ^{19}F NMR spectrum of **1**−OTf in CH_2Cl_2 shows three broad resonances at −69.7, −14.0, and 60.4 ppm (Figure 10 and Figure S5 for **2**). By comparison to the well-characterized iron(II) complexes of tfa ($CF_3CO_2^-$) with tmen and Me_3tacn,[16a] these three resonances can be assigned to free triflate, terminal triflate, and bridging triflate, respectively (as in **6** and **7** of Scheme 3). The selective substitution of only the terminal tfa ligands of $Fe_2(H_2O)(tfa)_4(tmen)_2$ indicated that the resonances of the bridging ligands are shifted further downfield as would

Scheme 3

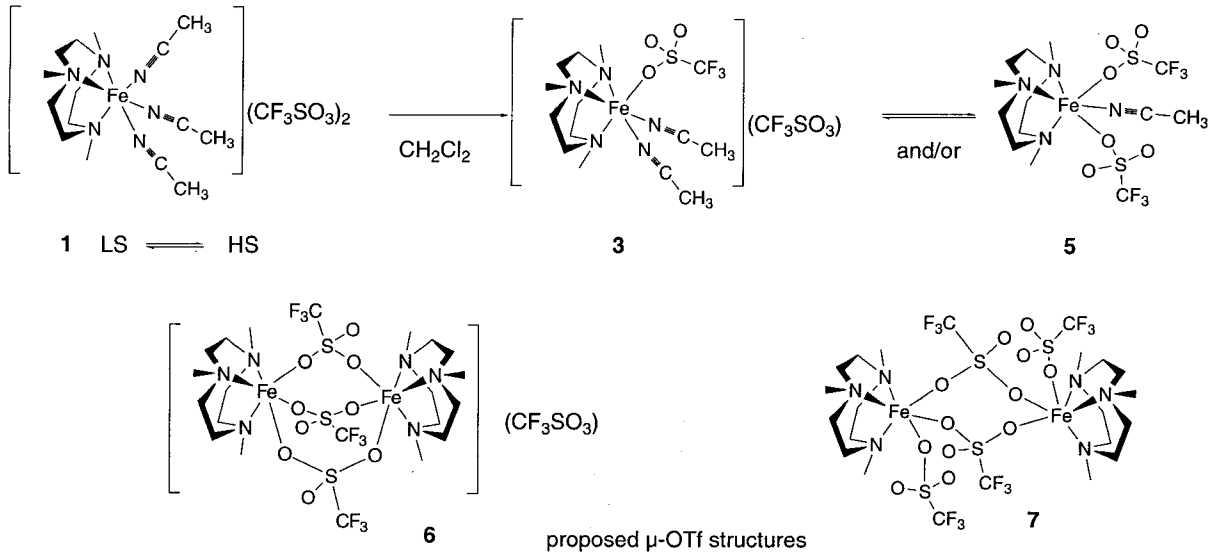

be expected by their proximity to two paramagnetic centers.[37] These bridging resonances are not as strongly shifted in the more strongly antiferromagnetically coupled μ-hydroxo dimer $[Fe_2(\mu\text{-OH})(\mu\text{-tfa})_2(Me_3tacn)_2](OTf)$. In the related triflate-bridged complex $[Fe_2(\mu\text{-OH})(\mu\text{-OTf})_2(Me_3tacn)_2](OTf)$, the resonances of bridging and uncoordinated triflates occur at -11 and -69 ppm, respectively. However, in the less strongly antiferromagnetically coupled complex, $[Fe_2(\mu\text{-OTf})(MeDA)(tacn)_2](OTf)$, the resonances of bridging and uncoordinated triflates in CD_3CN occur at 26 and -78 ppm, respectively.[38] The triflate adopts a bridging mode similar to that observed in $[Fe_2(\mu\text{-OTf})(Me_2DA)(MeOH)_2(MeIm)_3](OTf)$.[39]

When the CH_2Cl_2 solution of **1**$-$OTf is cooled below -50 °C, the free triflate resonance appears sharper and is only slightly shifted (Figure 10 and Table S4). The paramagnetically shifted ^{19}F resonances for coordinated triflates have shifted further downfield and split into a set of four bridging triflates between 160 and 100 ppm and two types of terminal triflates between 20 and 10 ppm. The presence of the acetonitrile as a competing ligand adds to the complexity of the low-temperature spectra (see Scheme 3). When the solution is warmed, the free triflate resonance broadens and becomes smaller in relation to the other peaks. This can be explained by a change in the equilibrium concentrations of the different species concurrent with a change of the exchange rate toward a value closer to the time scale of the NMR experiment. The four bridging triflate resonances are probably caused by distinct species that undergo slow exchange in solution. As the solution warms to room temperature, these resonances merge into the one sharp resonance at 60.4 ppm. At -80 °C there are two terminal triflate resonances that behave similarly to the bridging triflate resonances in that they broaden and collapse into one resonance at room temperature and above. There is also a shift in the population of the two species that contain terminal triflates as the temperature is increased.

To more clearly illustrate that these equilibria involve coordinated acetonitrile, a titration of acetonitrile into a solution of **2**$-$OTf was monitored by ^{19}F NMR at two temperatures (Supporting Information, Figures S6 and S7). The initial spectrum at 30 °C exhibits one sharp resonance at 56.5 ppm and two broad smaller resonances at -16 and -65 ppm. The former is likely to be caused by fast exchange between bridging and terminal triflates in a binuclear or polynuclear complex, whereas the two broad resonances are caused by slow exchange between terminal triflates on a mononuclear complex and uncoordinated triflate. The initial spectrum at -55 °C shows the complicated spectrum described above with the bridging triflates being the major species present and a significant amount of terminal triflates presumably because of more residual acetonitrile in the solid sample (Figures 10b and S5a). As acetonitrile is titrated into the solution, the equilibrium first shifts to favor the terminal triflates and finally the free triflate. Triflate-bridged species are seen at 30 °C with as many as 12 equiv of MeCN, but none are detectable with only 6 equiv of MeCN at -55 °C. A species such as **3** dominates in the presence of 24 equiv of MeCN at 30 °C, whereas only a small amount of coordinated triflate occurs at low temperature. This is consistent with the favorable formation of the LS ↔ HS complex **1**$-$OTf at low temperature.

The crystals of **2** that we have obtained that could contain bridging triflates have not been suitable for X-ray crystallographic studies. However, analogous carboxylate chemistry[16b,40] suggests that $[Fe_2(\mu\text{-OTf})_3(Me_3tacn)](OTf)$ may be one possibility (**6** in Scheme 3). Discrete Pt(IV) complexes, $tmenPtMe_3(OTf)$, $\{thfPtMe_3(OTf)\}_2$, and $\{PtMe_3(OTf)\}_4$ with terminal, μ_2-, and μ_3-triflates, respectively, are also potential structural types for the iron complexes in solution.[41] There is considerable crystallograpahic evidence for the role of triflate as a bridging ligand in the solid-state chemistry of Cu(I) and Ag(I).[42]

Conclusions

We have shown that under carefully controlled conditions one can synthesize a variety of highly reactive, substitutionally

(37) Hagen, K. S.; Lachicotte, R.; Kitaygorodskiy, A. *J. Am. Chem. Soc.* **1993**, *115*, 12617−12618.
(38) Hagen, K. S.; Elbouadilli, A.; Kitaygorodskiy, A. Unpublished results.
(39) Me_2DA is abbreviated as XDK in the following. Herold, S.; Pence, L. E.; Lippard, S. J. *J. Am. Chem. Soc.* **1995**, *117*, 6134−6135.
(40) Wieghardt, K.; Bossek, U.; Nuber, B.; Weiss, J.; Bonvoisin, J.; Corbella, M.; Vitols, S. E.; Girerd, J. J. *J. Am. Chem. Soc.* **1988**, *110*, 7398−7411.
(41) Schlecht, S.; Dehnicke, K.; Magull, J.; Fenske, D. *Angew. Chem., Int. Ed. Engl.* **1997**, *36*, 1994−1995.
(42) (a) Timmermans, P. J. J. A.; Mackor, A.; Spek, A. L.; Kojic-Prodic, B. *J. Organomet. Chem.* **1984**, *276*, 287. (b) Ferrara, J. D.; Tessier-Youngs, C.; Youngs, W. J. *Inorg. Chem.* **1988**, *27*, 2201−2202. (c) Nickel, T.; Porschke, K.-R.; Goddard, R.; Kruger, C. *Inorg. Chem.* **1992**, *31*, 4428−4430. (d) Hirsch, K. A.; Wilson, S. R.; Moore, J. S. *Inorg. Chem.* **1997**, *36*, 2960−2968.

labile, iron(II) complexes with the facially capping ligand Me_3-tacn. These complexes display interesting electronic properties, including LS ↔ HS crossover, when the $[(Me_3tacn)Fe]^{2+}$ moiety is coordinated by an additional three nitrile ligands to form the purple complex **1**. The bulkier butyronitrile enhances the HS components of solution equilibria relative to acetonitrile. Exclusively HS complexes form when one or more of the nitriles either are lost in the solid state or in solution or are replaced by other solvent molecules or triflates to form the crystallographically characterized structures **1**, **3**, and **4** of Scheme 1 and the other proposed structures in Schemes 2 and 3. ^{19}F NMR spectra confirm that the triflates coordinate in both bridging and terminal modes in methylene chloride to form binuclear or higher nuclearity complexes. The species that exist in methylene chloride solution do not necessarily have the same structure as the crystals that are isolated from methylene chloride.

The implication of binuclear or higher nuclearity complexes in methylene chloride has ramifications for the solution reactivity of these complexes with reagents such as dioxygen. The ability to make LS complexes with neutral monodentate ligands affords a system where photochemical control of reactivity may be possible. For instance, LS **1**−BPh_4 does not react when O_2 is bubbled overnight through a solution in the dark, but it readily reacts with O_2 when irradiated with visible light.[43]

Acknowledgment. This work was supported by grants from the National Institutes of Health (GM 46506 and S10 RR07323). We thank Dr. Zhang and Mr. Adam Rondinone of Georgia Institute of Technology for the solid-state magnetic susceptibility data.

Supporting Information Available: Labeled figures and crystallographic files (in CIF format) of **1**−BPh_4 (at −30 and 60 °C), **3**, and **4** and variable temperature NMR spectra and tables of **1**−PrCN (^2H), **2** in CH_2Cl_2 (^{19}F), and titrations of **2** in CH_2Cl_2 with MeCN at −55 and 30 °C. This material is available free of charge via the Internet at http://pubs.acs.org.

IC990584+

(43) Blakesley, D.; Hagen, K. S. Unpublished results.